Palacký University Olomouc

Bachelor Thesis

Olomouc 2019 **Martin Löffelmann**

Palacký University Olomouc

Faculty of Science

Department of Cell Biology and Genetics

Development and characterization of drug resistant cancer cell lines to the metal chelating compounds with selective anticancer activity

Bachelor Thesis

Martin Löffelmann

Study Programme: Biology

Field of Study: Molecular and Cell Biology

Form of study: Full-time

Olomouc 2019

Supervisor: Mgr. Vaishali Uniyal

Bibliographical identification

Name and surname of the author: Martin Löffelmann

Title: Development and characterization of drug resistant cancer cell lines to the metal chelating compounds with selective anticancer activity

Type of thesis: Bachelor

Department: Department of Cell Biology and Genetics, Faculty of Science, Palacký University Olomouc

Supervisor: Mgr. Vaishali Uniyal

Year of presentation: 2020

Abstract

Multidrug resistance in cancer represents a major challenge in anticancer therapy. This thesis is focused on the development of drug resistant cancer cell lines to understand the molecular mechanisms of drug resistance. Two metal chelators were used, XYZ and VLX600, with anticancer properties for developing drug resistance in HCT116 and CCRF-CEM cancer cell lines. VLX600 resistant HCT116 cell line was successfully developed with nine-fold increase in IC_{50} value. Characterization of those resistant cells showed higher expression of P-glycoprotein (Pgp) and Multidrug resistance-associated protein 1 (MRP1). Pgp and MRP1 belong to the ATP-binding cassette (ABC) transporters family and prevent accumulation of drugs within the cancer cell. Both metal chelators had low IC_{50} values and no resistance was developed in CCRF-CEM cell line. Metal chelating compounds have a potential to become anticancer drugs in combination with other therapies to overcome multidrug resistance.

Keywords: drug resistance in cancer, anticancer therapy, ABC transporters, metal chelators, VLX600

Number of pages: 50

Number of appendices: 1

Language: English

Bibliografické údaje

Jméno a příjmení autora: Martin Löffelmann

Název práce: Vývoj a charakterizace rezistentních nádorových linií vůči chelatačním činidlům se selektivní protinádorovou aktivitou

Typ práce: Bakalářská

Pracoviště: Katedra buněčné biologie a genetiky, PřF UP v Olomouci

Vedoucí práce: Mgr. Vaishali Uniyal

Rok obhajoby práce: 2020

Abstrakt

Mnohočetná léková rezistence u nádorů představuje významnou výzvu v protinádorové terapii. Tato práce je zaměřena na vývoj rezistentních nádorových buněčných linií k pochopení molekulárních mechanismů mnohočetné lékové rezistence. Byly použity dva chelátory železa, XYZ a VLX600, s protinádorovou aktivitou pro vývoj rezistence u buněčných linií HCT116 a CCRF-CEM. Rezistentní linie HCT116 vůči VLX600 byla úspěšně vyvinuta s devítinásobným nárůstem rezistence. Charakterizace těchto rezistentních buněk ukázala vyšší expresi P-glykoproteinu (Pgp) a Proteinu 1 spojeného s mnohočetnou lékovou rezistencí (MRP1). Pgp a MRP1 patří do rodiny transportérů vázajících ATP (ABC) a zabraňují akumulaci léčiv uvnitř nádorové buňky. Oba chelátory měly nízké hodnoty IC_{50} a u buněčné linie CCRF-CEM nebyla vyvinuta žádná rezistence. Chelatační činidla mají potenciál stát se protinádorovými léčivy v kombinaci s jinou léčbou k překonání mnohočetné lékové rezistence.

Klíčová slova: mnohočetná léková rezistence, protinádorová terapie, ABC transportéry, chelatační činidla, VLX600

Počet stran: 50

Počet příloh: 1

Jazyk: angličtina

Declaration

I hereby declare, that I elaborated this bachelor thesis independently under the supervision of Mgr. Vaishali Uniyal, using information sources referred in the References chapter only.

…….

Martin Löffelmann

ACKNOWLEDGMENT

I would like to thank my supervisor Mgr. Vaishali Uniyal for her guidance, patience and all theoretical and practical skills that I could learn from her. I am also very grateful to MUDr. Petr Džubák, Ph.D. for allowing me to work on my thesis at the Institute of Molecular and Translational Medicine and Bc. Renata Burianová for sharing her laboratory expertise in flow cytometry. I would also like to thank my wife and my family for their support during my studies.

The bachelor thesis was created with a financial support of the grant TE02000058, MOLDIMED.

Table of Contents

List of abbreviations

ABC transporters	ATP-binding cassette transporters
ATP	Adenosine triphosphate
BCRP	Breast cancer resistance protein
BSA	Bovine serum albumin
CYP	Cytochrome P-450
DFO	Desferrioxamine
DMSO	Dimethyl sulfoxide
EDTA	Ethylenediamine tetraacetic acid
FBS	Fetal bovine serum
FITC	Fluorescein isothiocyanate
GST	Glutathione-S-Transferase
IC_{50}	Half maximal inhibitory concentration
IgG	Immunoglobulin G
MDR	Multidrug resistance
MRP1	Multidrug resistance-associated protein 1
NO	Nitrogen monoxide
P/S	Penicillin/Streptomycin
PBS	Phosphate buffered saline
Pgp	P-glycoprotein
PI	Propidium iodide
RNAi	RNA interference
RNase	Ribonuclease A
ROS	Reactive oxygen species
RR	Ribonucleotide reductase
SD	Standard deviation
siRNA	Small interfering RNA
TF	Transferrin
TFR1	Transferrin receptor 1
UGT	5’-diphospho glucuronosyltransferase
WHO	World Health Organization

List of figures

List of tables

1 INTRODUCTION

This thesis focuses on the development and characterization of cancer cell lines against metal chelating compounds. Drug resistance in cancer is becoming a major problem during the cancer treatment. Previous studies described ways of how to develop drug resistance *in vitro* and which mechanisms are responsible for it. However, no research has yet described the mechanism of the drug resistance against metal chelators. Metal chelators are becoming new anticancer drugs with promising effects. But this thesis shows, that cancer cells may develop resistance even to novel compounds over time.

2 AIMS OF THE THESIS

- Finding IC_{50} values for selected metal chelating compounds
- Development of drug resistant cancer cell lines against selected metal chelating compounds
- Characterization of the drug resistant cell lines

3 THE CURRENT STATE OF KNOWLEDGE

3.1 Cancer statistics

Cancer is one of the most frequent causes of death in the world. According to the estimates of cancer incidence and mortality provided by the status report *GLOBOCAN 2018*, produced by the International Agency for Research on Cancer (IARC), the cases are rapidly growing worldwide (1). Another reason why cancer is a major medical issue is that it is a leading cause of premature death, mainly in the most developed countries (e.g. Europe, North America, Japan, Australia) (**Fig. 1**).

According to the World Health Organization (WHO) cancer is responsible for estimated 9.6 million deaths in 2018. The incidence rate estimates around 18.1 million. The most common types of cancer for men and women are lung cancer (11.6% of the total cases), followed by female breast cancer, colorectal cancer and prostate cancer. The leading cause of cancer death among men is lung cancer, followed by liver and stomach cancer. Among women it is breast cancer, followed by lung and colorectal cancer (1).

Unfortunately, the Czech Republic belongs to the top 10 countries with the highest incidence rate of kidney (4^{th}) and pancreatic (8^{th}) cancers (2). Kidney cancer is a metabolic disease, whose therapy consists of targeting certain metabolic pathways. However, patients develop resistance and progress of the disease (3). Pancreatic cancer is one of the most aggressive types of cancer and most of the patients are diagnosed at an advanced stage of the disease (4).

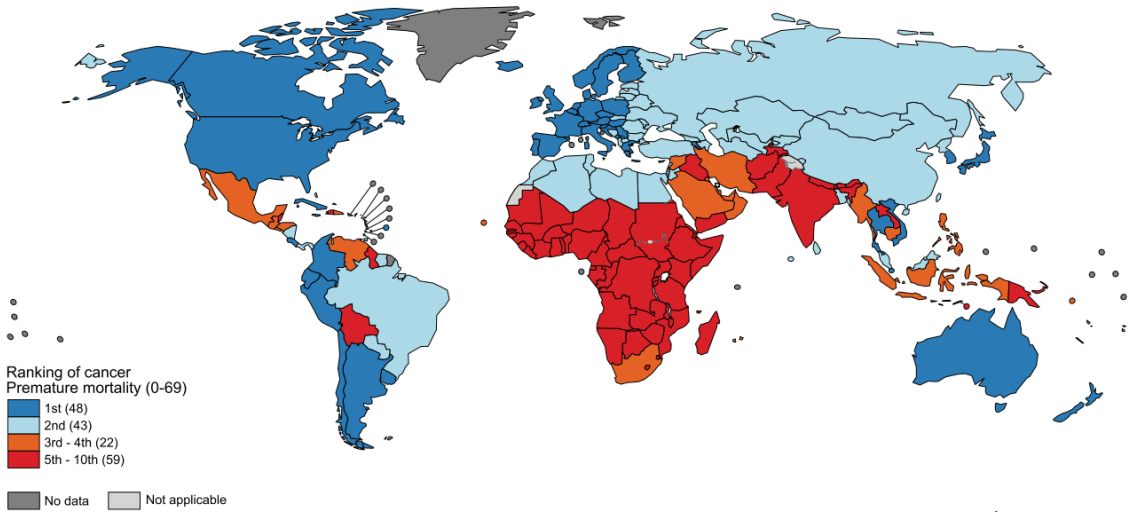

Figure 1: Map presenting the ranking of cancer as a cause of premature death at age below 70 in 2015. *Source: WHO*.

3.2 Role of iron in cancer

Iron is an essential element involved in many important cellular processes. It is a part of mitochondrial enzymes, DNA synthesis and cell cycle enzymes, detoxification enzymes and it is also a vital part of haemoglobin, which is responsible for oxygen transport in bloodstream.

Iron also participates in free radical-generating reactions, i.e., reactive oxygen species (ROS) and hydroxyl radicals. It is possible due to Fenton reaction, in which ferrous iron (Fe^{2+}) reacts with hydrogen peroxide and produces hydroxyl radical. The oxidized iron can be reduced back to ferrous iron in the presence of superoxide (5). ROS are toxic for cells, because of their ability to cause oxidative damage to DNA, lipids and proteins. They even cause strong DNA base alterations of guanine and thymine and strand breaks (6). In other words, the role of iron is ambivalent.

Iron circulates in bloodstream in the form of ferric ion (Fe^{3+}) and is conjugated to transferrin (TF), which binds two ferric atoms. TF and two bound iron atoms are transported through a transferrin receptor 1 (TFR1) on a cell membrane into the cell. This complex TF-[Fe^{3+}]-TFR1 travels into an endosome. The acidic environment of the endosome releases the ferric ions, which are reduced to ferrous ions (Fe^{2+}). These atoms are harmless for the cell and are transported out of the endosome into a cytoplasm. Then they are incorporated into any metabolic processes where they play a crucial role (DNA and haem synthesis, oxidative phosphorylation in mitochondria, etc.). Cells store excess iron in the form of ferrous ions (Fe^{2+}) thanks to the iron storage protein called ferritin.

Important cellular iron-dependent processes are not only a part of normal cells but are equally important in cancer cells. Tumour cells are even capable of reprogramming the iron metabolism. One of these mechanisms were recently identified as iron efflux pumps called ferroportin-hepcidin regulatory axis (**Fig. 2**). These pumps were discovered on the surface of enterocytes, macrophages and hepatocytes (7). Hepcidin is a peptide hormone which binds to the efflux pump ferroportin and regulates its expression. The synthesis of hepcidin is induced by an excess iron. Ferroportin as an iron efflux pump is responsible for transporting iron out of the cell in conjunction with an oxidase (ceruloplasmin or hephaestin) which can re-oxidize iron.

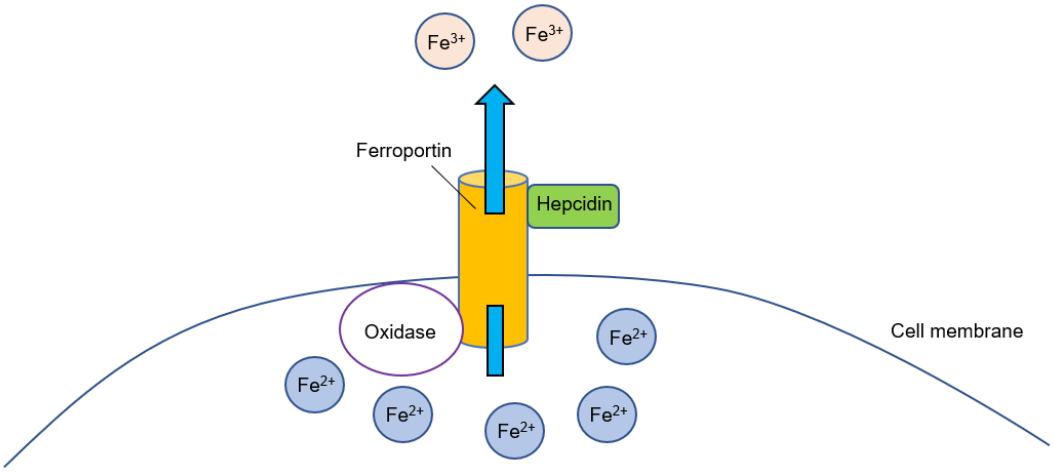

Figure 2: Ferroportin-hepcidin axis transporting ferrous ions out of the cell. Hepcidin binds to the efflux pump ferroportin and regulates its expression. The ferrous ions are oxidized by ceruloplasmin or hephaestin to ferric ions during transportation.

Tumours contain a special environment in terms of metabolism, including iron metabolism. There is an increased expression of TFR1 and hepcidin and low levels of ferroportin in cancer cells. As a result, the concentration of iron in tumour is increased (8).

Another form that tumour cells release iron is *via* the signalling molecule nitrogen monoxide (NO). This iron efflux requires glutathione. Interestingly, this NO-dependent release has been identified to work in conjunction with the multidrug resistance-associated protein 1 (9), which is usually responsible for drug resistance in cancer (10,11).

3.3 Iron chelators in cancer therapy

3.3.1 Potential targets

The iron chelation therapy was at first used in iron toxicity overload diseases, but as the role of iron in tumour is very important and is involved in many metabolic processes, efforts have been made to use iron chelators in cancer therapy as well. Consequently, tumour will suffer from iron deficiency and its lifespan will decrease.

One of the targets that has been picked for iron chelators is enzyme ribonucleotide reductase (RR). Its main function is to convert ribonucleotides into deoxyribonucleotides for DNA synthesis. This enzyme requires two things to work properly: oxygen and iron (12). Therefore, iron chelators are mainly used as RR inhibitors.

Another target for iron chelators is the TFR1. As mentioned before, cancer cells contain higher expression of TFR1 and high concentration of iron in cytoplasm. If iron chelators would inhibit this iron intake via TFR1, tumour growth would be supressed (13).

Iron depletion by chelators also affects the cell cycle by decreasing cyclins which bind with cyclin-dependent kinases (14). The results of this action lead to G_1/S phase suppression.

A very important role in cancer cells shows a tumour suppressor protein p53. Its main purpose is an induction of apoptosis if damage changes to cell are irreversible and it also serves as a cell cycle checkpoint. Tumour cells often disable this protein, which prevents the induction of apoptosis (15). A possible solution for this problem may offer iron chelators. Cancer cells incubated with chelators showed up-regulated expression of p53, which remained elevated for 24 hours. Tumour growth inhibition was observed as well (16).

3.3.2 Clinically approved iron chelators with anti-proliferative activity

Desferrioxamine (DFO) (**Fig. 3**) is a hexadentate chelator with a high affinity for iron, which makes it an excellent therapy for the treatment of iron overload diseases. However *in vitro, in vivo* studies and clinical trials in neuroblastoma patients showed sensitivity to iron chelation therapy provided by DFO (17). DFO also shows anti-proliferative activity against other types of tumours. For example, lymphoid leukemia (18) or hepatocellular carcinoma in animal models (19). The mechanism of action of this compound is RR-inhibition. In addition, it also affects the expression of mitochondrial enzymes such as citrate synthase, isocitrate dehydrogenase and succinate dehydrogenase that are suppressed because of the iron depletion caused by DFO (20). There are also some negatives about this drug. Some studies failed to detect any anti-proliferative effects *in vivo* (21), which could be due to short half-life and poor absorption from the gut (22).

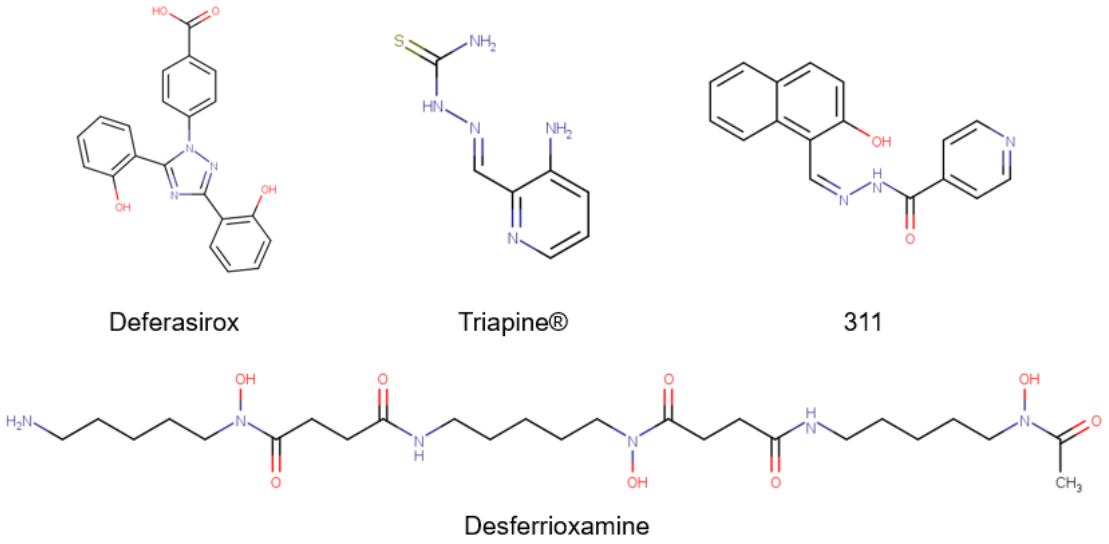

Figure 3: Molecular structures of metal chelators with anti-proliferative activity.

Deferasirox (**Fig. 3**) belongs to a group of synthetic iron chelators. In an attempt to increase efficacy and reduce adverse effects, it successfully passed the clinical trials (23). Deferasirox shows an anti-tumour activity in myeloid leukemia and in lymphoma cells, moreover its significant advantage is that it is administered orally (24,25). All this information suggests that deferasirox may be a potential anticancer drug, however, further research is needed.

3.3.3 Thiosemicarbazones

Thiosemicarbazones are an important group of iron chelators. In addition to their high affinity for iron and copper, these compounds also show an anticancer activity. The mechanism of action in tumour cells is DNA synthesis inhibition including RR (13). One of the most promising and well-studied compounds that even reached the clinical trials was Triapine® (**Fig. 3**). It is administered alone or in combination with other therapeutics mainly to patients with leukemia and kidney cancer. But it also showed a lot of adverse effects like anaemia, hypoxia, hypotension, fatigue, nausea and vomiting (26). Unfortunately, low efficacy and low patients respond led to a premature termination of clinical trials (27). Despite its promising results from *in vivo* studies and synergistic inhibitory effects with other therapeutics, Triapine® will probably not be used as an anticancer drug in the future.

Chelators derived from pyridoxal isonicotinoyl hydrazone have also been tested for their anti-proliferative activity. Iron chelator 311 (2-hydroxy-1-naphthylaldehyde benzoyl hydrazone) (**Fig. 3**) possesses a much higher iron affinity and even an anti-proliferative activity in comparison to DFO. RR-inhibition was observed in the CCRF-CEM (T-lymphoblastic leukemia) cell line. Due to a lipophilic character of 311, which allows easier access through cell membranes, the intracellular iron pool is open for chelation. A low IC_{50} (0.28 μM in CCRF-CEM cell line) may serve as an evidence of a significant anti-proliferative activity (28). Molecules involved in cell-cycle control may also be affected by 311 as well as a p53 increase (29).

3.3.4 VLX600 as a promising novel iron chelator

VLX600 (**Fig. 4**) is an iron chelator that differs from other chelators in one thing, that is, it does not generate ROS. The mechanism of action is a depletion of intracellular iron pools which leads to a reduced mitochondrial respiration. The impaired oxidative phosphorylation results in bioenergetic catastrophe followed by tumour death. A cytochrome oxidase activity decrease was observed during studies as well (30,31). The properties that make this compound interesting as a potential anticancer drug are its lipophilicity, low IC_{50} values (~1 $\mu mol \cdot l^{-1}$) *in vitro*, positive tolerance in animal models and finally that VLX600 has already reached the clinical trials. Patients with colon, prostate, pancreas, breast, hepatocellular, uterine and other tumours were involved in the phase I clinical study. Several adverse effects like nausea, vomiting, fatigue or decreased appetite were reported. A positive response was reported among 32% of the patients, and overall, the drug was well tolerated (32). Further studies are expected to determine the use of VLX600 as a potential iron chelator in oncological treatment.

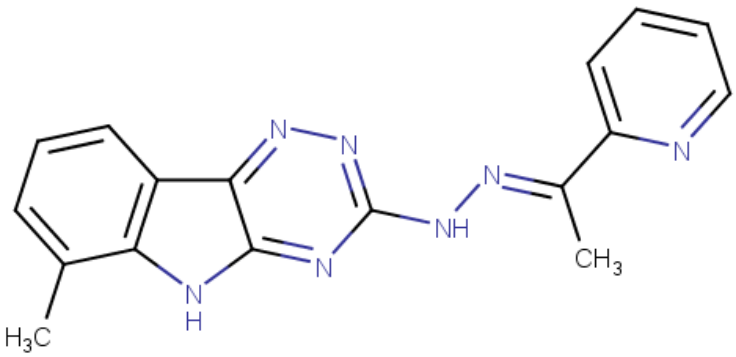

Figure 4: Molecular structure of a novel VLX600 iron chelator.

3.4 Cancer resistance

3.4.1 Types of resistance

Drug resistance is a phenomenon that occurs when disease becomes tolerant to a conservative treatment. It was first described in bacteria that developed antibiotic resistance. Unfortunately, this concept may also develop in cancer cells and lead to cancer relapse and death. Since this topic represents a major clinical problem it has been intensively studied and is referred to as multidrug resistance (MDR).

There are many categories of MDR in cancer and the four most studied will be described below (**Fig. 5**). Other ways, how cancer cells develop drug resistance, are DNA damage repair, cell death inhibition or epigenetic changes (33). Some of the mechanisms are tumour-specific, while others (P-glycoprotein) are generally present in healthy cells where they perform vital functions. The understanding of the ways of cancer resistance is an important task, the fulfilment of which will result in a more effective therapy and improved clinical outcomes.

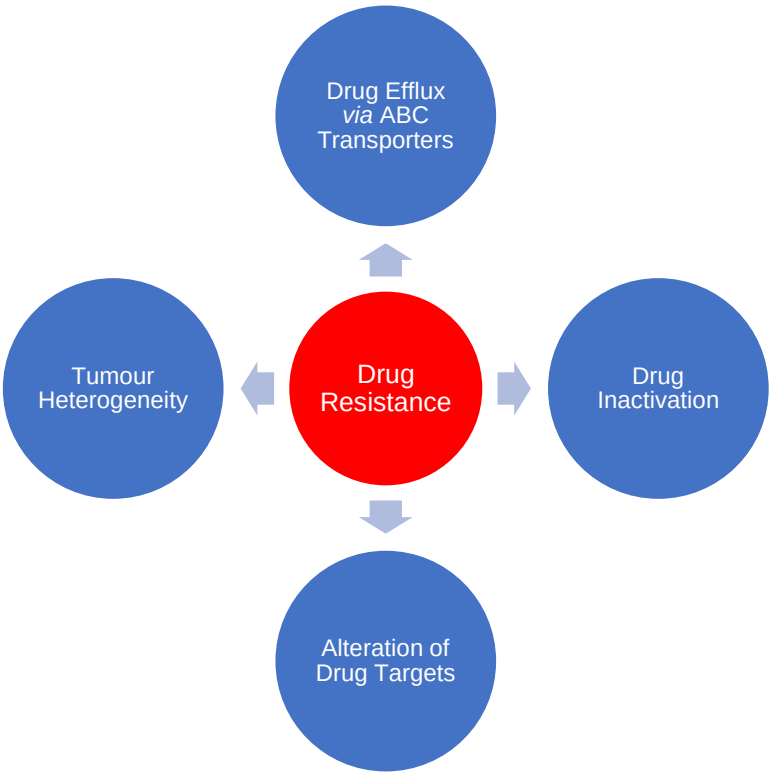

Figure 5: Diagram illustrating the basic types of drug resistance in cancer. The mechanisms can act independently or in combination.

3.4.2 Drug Efflux *via* ABC Transporters

The ATP-binding cassette (ABC) transporters are responsible for the MDR mechanism, which involves the transport of xenobiotics out of the cell, thereby preventing the accumulation of anticancer drugs within the cancer cell. The transporters consist of four domains, namely two transmembrane and two nucleotide. Upon binding of a substrate to the transmembrane domain, the energy released from ATP hydrolysis changes the conformation of the transporter, resulting in removal of the substrate from the cell (34). The main transporters responsible for the MDR in cancer are multidrug resistance protein 1 (MDR1), multidrug resistance-associated protein 1 (MRP1) and breast cancer resistance protein (BCRP) (10).

MDR1 gene, physiologically present in colon and liver, produces P-glycoprotein (Pgp) which works as a drug efflux pump. During cancer, an overexpression of *MDR1* occurs, and provides resistance to a wide sort of anticancer drugs (e.g., taxanes, *Vinca* alkaloids or anthracyclines) (35).

MRP1 is located in the plasma membrane and its overexpression results in MDR to the same drugs as MDR1 except for taxanes (36). Similarly, BCRP is also mainly present in the cell membrane and is responsible for MDR in breast cancer, colon, ovarian and gastric carcinomas (37).

3.4.3 Drug Inactivation

The use of conventional cancer therapy involves metabolic pathways that the drugs need to undergo to achieve a desired effect. However, these pathways are usually blocked or changed during MDR in cancer. For example, acute myelogenous leukemia is treated with cytarabine. This compound must first be phosphorylated in order to be pharmacologically active. Preventing it leads to a cytarabine resistance (38). The systems involved in such alterations are very important for the cell, because they inactivate xenobiotics that can be toxic.

These systems include glutathione-S-transferase (GST) and uridine 5’-diphospho glucuronosyltransferase (UGT) superfamilies. Both are responsible for inactivation of environmental carcinogens and act as detoxifying enzymes. Nevertheless, the elevation of GST enhances undesirable detoxification of anticancer drugs and lower regulation

of genes coding UGT occur in certain tumours (39). These changes in enzyme activity lead to MDR.

Probably one of the most studied cellular systems responsible for xenobiotics metabolism and inactivation is cytochrome P450 (CYP). In mammals, eighteen CYP families are known, but only three of them are responsible for xenobiotic metabolism. The rest plays a role in the metabolism of steroids and fatty acids. In tumour cells, an elevated activity of CYPs (groups CYP1A, CYP2C and CYP3A) was observed, which leads to the inactivation of anticancer drugs. However, CYP1B1 expressed protein relates to metastasis and colon adenocarcinoma, but is also expressed at low levels in healthy tissue (40,41). This fact can serve as a proposal for the development of a targeted therapy in cancer, both genetic and conservative therapies.

3.4.4 Alteration of Drug Targets

The efficiency of an anticancer drug depends on the molecular target of a tumour. This may include a vital enzyme, DNA synthesis, inhibition of mitotic processes, etc. Alteration of these targets, such as mutations or modifications, has a significant effect on the pharmacological result and may eventually lead to a drug resistance.

One of these targets represents topoisomerase II, an enzyme involved in the process of replication. The human leukemia cell line HL-60/AMSA possesses at least 50-fold higher resistance to amsacrine which inhibits topoisomerase II. This resistance is caused by a single base mutation in the enzyme gene (42).

Unfortunately, even a targeted therapy is a subject to resistance mechanisms. The development of resistance was observed during the treatment of chronic myeloid leukemia with tyrosine kinase inhibitors (Imatinib). MDR was associated with a single amino acid substitution in a threonine residue of the Abl kinase domain. This change led to a creation of an important bond with the drug (43). That means that the targeted therapy can lose its effectiveness just like a conventional treatment.

3.4.5 Tumour Heterogeneity

Tumour usually does not consist of a homogenous population of cancer cells. Some of the cells exhibit the characteristics of stem cells and these mainly develop the drug resistance. Therefore, only the sensitive cells of the tumour are killed during

the treatment and the drug resistant ones survive. Eventually there is a risk, that the resistant cells will form metastasis.

Using comparative genomic hybridization in breast cancer revealed monogenomic and polygenomic types of tumours (44). A monogenomic structure is more sensitive to the anticancer drugs while the polygenomic contains different subpopulations of the cells and in addition, it may exhibit the mechanisms of resistance mentioned above.

Pancreatic cancer is another type that possesses high drug resistance due to tumour heterogeneity, which is both between tumours and within the tumour itself. Heterogeneity develops in the early stage and may eventually lead to metastasis. This combination of drug resistance, tumour heterogeneity and metastatic complications makes the pancreatic cancer of the most deadly malignancies resulting in high mortality rates (45).

3.4.6 Overcoming the multidrug resistance in cancer

There are several therapeutic ways that focus on MDR in cancer. One of the best studied is the inhibition of ABC transporters, mainly Pgp. The first generation of ABC modulators -verapamil, cyclosporine A, quinine- was not efficient during clinical trials and some of the compounds showed toxicity. The second generation -valspodar and biricodar- showed higher efficiency and was combined with a conventional therapy. However, poor outcomes during clinical trials and inhibition of CYP in healthy tissue resulted in a decreased metabolism of the drugs and therefore high toxicity. The third generation is focused on very low concentrations (nanomolar scale) and extremely high efficiency in comparison to the first two generations. Tariquidar, zosuquidar and elacridar belong into this group. The first two showed promising results in clinical trials (11,46). An interesting fact is that most of the ABC inhibitors can inhibit specifically Pgp and no other transporters. Therefore, analogues of tariquidar were prepared, that focus on the MRP1 inhibition (47).

Using natural compounds is another form of overcoming MDR. Curcumin as NFκB inhibitor (48) and ABC modulator (49) as well makes this compound very interesting. NFκB serves as a transcriptional nuclear factor responsible for apoptosis, cell proliferation and MDR. Flavonoid quercetin possesses antioxidant and antitumor effects. The synergistic effect was investigated by Choi *et al* using quercetin as a Pgp inhibitor

and the bioavailability of anticancer drug doxorubicin administered in rats. Due to Pgp inhibition an increase of orally administered doxorubicin metabolism was reported (50).

Another innovative strategy is RNA interference (RNAi). It serves as a cellular defense by destroying a specific mRNA and thus preventing the expression of unwanted genes. This is achieved by a small interfering RNA (siRNA) which binds to the target mRNA that is cleaved and destroyed by the cell. The purpose of RNAi in cancer therapy consists in using synthetic siRNAs for down-regulation of Pgp or other ABC transporters. Reduction of resistance in the cell lines was observed as a result (51).

A modern way to overcome or circumvent MDR is the use of nanoparticles. They are widely used as anticancer drug carriers in targeted therapy, show low toxicity and high efficiency at low concentrations. There are mainly three ways how nanoparticles can improve MDR therapy: 1. they can bypass ABC transporters and the drug efflux because they enter the cells *via* endocytosis, 2. an ability to enhance the solubility of hydrophobic compounds and providing long controlled release of the drug, and 3. nanoparticles may serve as carriers for both conventional therapeutics and ABC modulators (35). Targeted nanocarriers have a potential to significantly improve MDR therapy combining multiple approaches, but further research and improvement is needed to achieve positive clinical outcomes.

4 MATERIALS AND METHODS

4.1 Materials

4.1.1 Biological material

For the development of drug resistance these cancer cell lines were used:

- HCT116 – Organism: *Homo sapiens*, human; Tissue: colon; Disease: colorectal carcinoma; Culture Properties: adherent; Morphology: epithelial; ATCC® CCL-247™
- CCRF-CEM – Organism: *Homo sapiens*, human; Tissue: peripheral blood; Disease: acute lymphoblastic leukemia; Cell Type: T lymphoblast; Culture Properties: suspension; Morphology: lymphoblast; ATCC® CCL-119™

4.1.2 List of equipment, chemicals and machines

List of equipment

- Automatic pipettes, Research Plus (0,5–5 000 µl, Eppendorf)
- Battery powered pipette filler, Pipetus® (Hirschmann)
- Cell scrapers (TPP)
- Centrifuge tubes (50 ml, TPP)
- Eppendorf Safe-Lock Tubes (1.5 ml, Eppendorf)
- Filtermax rapid bottle-top filter (500 ml, TPP)
- Multi-channel pipette (10–100 µl, Eppendorf)
- Serological pipettes (10 ml, TPP)
- Test flow cytometry tubes (5 ml, BD Falcon)
- Tissue culture dishes (96x21 mm, growth surface 60 cm^2, TPP)
- Tissue culture flasks (75–150 cm^2, TPP)
- Tissue culture test plates (6, 96-well, TPP)

List of chemicals

- 10X PBS
- 70% Ethanol
- 100% Methanol

- Bovine Serum Albumin (BSA), pH 7, ≥ 98%, Catalog No. A7906 (Sigma-Aldrich)
- CellWASH, Catalog No. 349524 (BD Biosciences)
- Dimethyl Sulfoxide (DMSO) Cell culture grade (PanReac AplliChem)
- Ethylenediamine tetraacetic acid disodium salt dihydrate (EDTA), Catalog No. 11280 (Serva)
- FC Receptor saturation reagent, Catalog No. 732802 (BD Biosciences)
- Fetal Bovine Serum (FBS), Catalog No. 10270 (Gibco)
- McCoy's 5A Medium, with L-Glutamine (Diagnovum)
- MTS [3-(4,5-dimethylthiazol-2-yl)-5-(3-carboxymethoxyphenyl)-2-(4-sulfo-phenyl)-2H-tetrazolium, stock solution 8.5 mol · l^{-1} in 1x PBS, (Promega)
- Nonidet^{TM} P40 (NP-40) Substitute, Catalog No. 74385 (Sigma-Aldrich)
- Penicillin-Streptomycin antibiotics (P/S), Catalog No. P4333 (Sigma-Aldrich)
- Permeabilization solution 2, Catalog No. 340973 (BD Biosciences)
- Propidium iodide (PI), Catalog No. P4170 (Sigma-Aldrich)
- Purified water
- Ribonuclease A (RNase) from bovine pancreas, Catalog No. R5503 (Sigma-Aldrich)
- RPMI 1640 Medium, with L-Glutamine (BioWhittaker, Lonza)
- Sodium azide, Catalog No. S2002 (Sigma-Aldrich)
- Triton^{TM} X-100, Catalog No. T8787 (Sigma-Aldrich)
- TrypLE^{TM} Select Enzyme (1X) no phenol red, Catalog No. 11598846 (Gibco)
- VLX600 Iron Chelator (Calbiochem)
- XYZ Iron Chelator

List of antibodies

P-glycoprotein analysis

- Primary Antibody: Monoclonal Anti-P-Glycoprotein antibody produced in mouse, Catalog No. P7965 (Sigma-Aldrich)
- Isotype Control: IgG1 Isotype Control from murine myeloma, Catalog No. M5281 (Sigma-Aldrich)

- Secondary Antibody: Anti-Mouse IgG F(ab')$_2$ fragment-FITC antibody produced in sheep, Catalog No. F2883 (Sigma-Aldrich)

Multidrug resistance protein 1 analysis

- Primary Antibody: Monoclonal Antibody to MRP1 (Human) MRPm5, Catalog No. 801-012-C250 (Alexis Biochemicals)
- Isotype Control: IgG2a Isotype Control from murine myeloma, Catalog No. M5409 (Sigma-Aldrich)
- Secondary Antibody: Anti-Mouse IgG F(ab')$_2$ fragment-FITC antibody produced in sheep, Catalog No. F2883 (Sigma-Aldrich)

Phosphorylation of Histone H3P^{Ser10} analysis

- Primary Antibody: Anti-phospho-Histone H3 (Ser10) Antibody, Catalog No. 06-570 (Sigma-Aldrich)
- Secondary Antibody: Goat anti-Mouse IgG Secondary Antibody Alexa Fluor 488, Catalog No. A28175 (Thermo Scientific)

List of machines

- Analytical balance, SBC 21 (Scaltec)
- Cell Viability Analyzer Vi-Cell XR (Beckman Coulter)
- Centrifuge, 420R Rotina (Schoeller)
- Flow Cytometer, FACS Calibur (Becton Dickinson)
- Fluorescence Inverted Microscope IX51 (Olympus)
- Incubator CO_2, CO-170P-230 (New Brunswick Scientific)
- Laminar Box, MSC Advantage (Thermo Scientific)
- Multimode Plate Reader, EnVision (PerkinElmer)
- Thawing System, CTF2 (Biocision)
- Thermoblock, TS-100C (Biosan)
- Vortex-Genie 2 (Scientific Industries)
- Waterbath, WNB (Memmert)

4.1.3 List of solutions

Solutions and Media

1x PBS: 50 ml 10x PBS + 450 ml purified water, mix together and filter using vacuum

CCRF-CEM complete medium (10% FBS, 1% P/S): 500 ml RPMI 1640 Medium with L-Glutamine + 56 ml FBS + 5.6 ml P/S, mix together and filter using vacuum

HCT116 complete medium (10% FBS, 1% P/S): 500 ml McCoy's 5A Medium with L-Glutamine + 56 ml FBS + 5.6 ml P/S, mix together and filter using vacuum

Solutions and reagents for flow cytometry analysis

P-glycoprotein (Pgp) analysis

1x Permeabilising solution: 9 ml RNA water + 1 ml Permeabilization solution 2

Blocking solution: 50 mg BSA dissolve in 10 ml CellWASH with stirring

FC Receptor saturation reagent solution: 70 µl FC Receptor saturation reagent + 210 µl blocking solution

Isotype control: 7.1 µl isotype control IgG1 + 1 000 µl blocking solution added on ice; dilution factor 1:140.8

Primary antibody: 0.4 µl Monoclonal Anti-P-Glycoprotein antibody produced in mouse + 100 µl blocking solution added on ice; dilution factor 1:250

Rinse buffer: 500 mg BSA dissolve with stirring in 100 ml CellWASH and add 100 µl NP-40

Secondary antibody: 0.4 µl Anti-Mouse IgG $F(ab')_2$ fragment-FITC antibody produced in sheep + 100 µl blocking solution added on ice; dilution factor 1:250

Multidrug resistance protein 1 (MRP1) analysis

1x Permeabilising solution: 9 ml RNA water + 1 ml Permeabilization solution 2

Isotype control: 1.5 µl isotype control IgG2a + 300 µl rinse buffer added on ice; dilution factor 1:200

Primary antibody: 1.5 µl Monoclonal MRP1 Antibody + 300 µl rinse buffer added on ice; dilution factor 1:200

Rinse buffer: 0.25 g BSA dissolve with stirring in 50 ml 1x PBS and add 0.5 ml of 10% sodium azide

Rinse buffer incl NP-40: 50 µl NP-40 dissolve with stirring in 50 ml rinse buffer

Secondary antibody: 2 µl Anti-Mouse IgG F(ab')$_2$ fragment-FITC antibody produced in sheep + 498 µl rinse buffer incl NP-40 added on ice; dilution factor 1:250

Phosphorylation of Histone H3P^{Ser10} analysis

PBS + 0.25% Triton X-100: 2.5 ml of Triton X-100 dissolve in 1 l of 1x PBS

PBS + 1% FBS: 10 ml of FBS dilute in 1 l of 1x PBS

Primary antibody: 2 µl Anti-phospho-Histone H3 (Ser10) Antibody diluted in 998 µl 1x PBS + 1% FbS on ice; dilution factor 1:500

Propidium iodide solution: 14 mmol · l^{-1} in 1x PBS

RNase solution: 0.7 mmol · l^{-1} in 1x PBS

Secondary antibody: 2 µl Goat anti-Mouse IgG Secondary Antibody Alexa Fluor 488 diluted in 998 µl 1x PBS + 1% FbS on ice; dilution factor 1:500

4.2 Methods

4.2.1 Finding the IC_{50} values for iron chelators

For developing the drug resistant cancer cell lines two iron chelators were selected: VLX600 and XYZ iron chelator. VLX600 was diluted in DMSO to prepare a stock solution with a concentration of 30 mmol · l^{-1}. XYZ was diluted in DMSO as well and the stock solution had a concentration of 10 mmol · l^{-1}.

For finding the IC_{50} values MTS assay was performed. For CCRF-CEM cells a suspension with a concentration of 0.15 · 10^6 cells · ml^{-1} was prepared. CCRF-CEM cells were seeded 13 500 cells per well in a 96-well plate. The suspension of HCT116 cells had a concentration of 62 500 cells · ml^{-1}. HCT116 cells were seeded 5 600 cells per well. In a 96-well plate one column of wells was filled with 100 µl of complete medium as a blank. In the rest of the wells 90 µl of cell suspension were added. The plate was put into an incubator for 24 hours. None of outer wells were used for analysis.

After incubation 10 µl of 1.6% DMSO diluted in a complete medium were added to all wells in the second column of the plate as a control. A dilution series of the iron chelators were prepared in another 96-well plate. Stock solutions were diluted to prepare a concentration of 50 µmol · l^{-1}. A dilution factor was 1:4 in a descending order and 6 concentrations of a diluted drug were prepared in total. Final concentrations were 50, 12.5, 3.125, 0.78, 0.195 and 0.049 µmol · l^{-1}. Second prepared diluted series had a dilution

factor 1:4 and the concentrations were 25, 6.25, 1.6, 0.4, 0.1 and 0.025 μmol · l^{-1}. Third diluted series had a dilution factor 1:2. Prepared concentrations were 1, 0.5, 0.25, 0.125, 0.06 and 0.03 μmol · l^{-1}. Concentrations were chosen to cover multiplies of IC_{50} values. 10 μl of diluted drug solutions were added to the wells with cell suspensions in triplicates in the 96-well plate. The plate was incubated at 37 °C. After 48 hours of incubation, 15 μl of MTS solution were added to the whole plate. After 2 hours of incubation, absorbance was measured at 490 nm. MTS assay was performed three times to calculate the standard deviation (SD).

4.2.2 Development of drug resistant cancer cell lines

When the IC_{50} values were found, they were used to develop resistant cancer cell lines. During passaging two 150 cm^2 flasks with 5 million cells in each, with a viability of 95% or higher, were prepared. For cell viability and cell count analysis Cell Analyzer Vi-Cell was used. Flask 1 with a confluency of 50%, was treated with double concentration of IC_{50} (2x). Flask 2 with a confluency of 70% was treated with fivefold concentration of IC_{50} (5x) (**Fig 6**).

After a visible decrease in confluency to ~25%, the medium containing drug was removed, cells were washed with a complete medium. This pulse treatment was performed on both cell lines and for both iron chelators. When the cells started proliferating in the presence of the drug (attaining > 60% confluency), the drug treatment was increased by one unit of IC_{50}.

When the drug resistant clones showed certain signs of resistance, MTS assay was performed to determine a specific concentration of the drug to which the cells were resistant. This assay was performed three times in order to calculate SD.

Both parental and drug resistant cell lines were tested every two weeks for Mycoplasma contamination using qPCR method. In case of a positive result, the contaminated cell line was destroyed immediately. One of the negative control tests is shown in the Appendix part of this thesis.

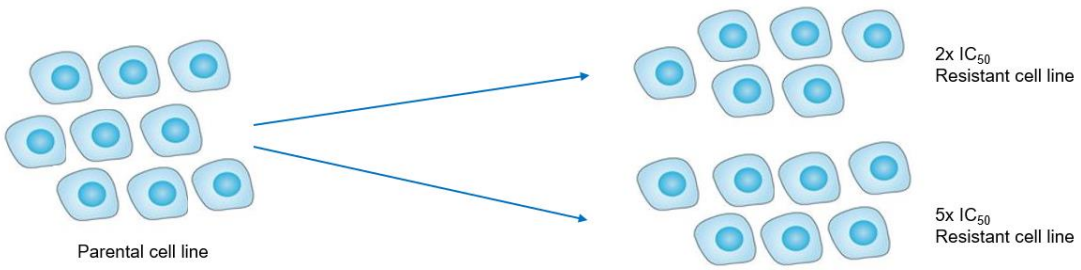

Figure 6: Diagram showing the way in which drug resistance was developed in both cell lines. Pulse treatment was used for both iron chelators.

4.2.3 Characterization of drug resistance against iron chelators

The characterization of drug resistance was done using flow cytometry. Three assays were performed: Pgp, MRP1 and Phosphorylation of Histone H3P^{Ser10} detection. The cells had to be prepared and fixed before measurements. All measurements were performed on both drug resistant and parental cells and both treated and untreated cells. Cytometry measurements were performed three times in order to calculate SD.

To perform cell fixation, it was necessary to prepare the cells. During passaging a cell suspension containing 1 million cells was added into a 60 cm^2 Petri dish with 12 ml of a complete medium. When the confluency reached ~70%, fixation was performed. For the measurements of treated cells, drug was added 24 hours before fixation.

For Pgp and MRP1 assays fixation process was the same. Medium from Petri dishes was transferred into 50 ml centrifuge tubes. Cells were washed with 3 ml of 1x PBS, which was after washing added to the removed medium. Then 3 ml of 4% EDTA in 1x PBS solution were added and the Petri dishes were put into an incubator for 15 minutes. After incubation 3 ml of complete medium were added. Cell suspension was mixed several times and transferred into the centrifuge tube with medium and PBS. Complete medium was added to the total volume of 20 ml. 500 µl was used for cell viability analysis using Vi-Cell. Centrifugation at 4 °C, 800 *g*, for 5 minutes. Medium was removed and the pellet was resuspended in 10 ml of 1x PBS. Centrifugation at 4 °C, 800 *g*, for 5 minutes. PBS was removed and the pellet was resuspended in 10 ml of methanol added drop by drop while the centrifuge tube was placed on vortex, set on a minimal setting. Cell suspensions were stored in a freezer at -20 °C. For Phosphorylation of Histone H3P^{Ser10} assay the fixation protocol was the same as for Pgp or MRP1, except that the 4% EDTA in 1x PBS solution was substituted with TrypLE^{TM}.

4.2.3.1 Pgp analysis

For Pgp analysis three samples from frozen stock cell suspension were prepared, each containing 1 million cells. Cell suspensions were transferred into cytometry tubes. Samples were centrifuged at room temperature, 500 *g* for 5 minutes (these centrifugation parameters were the same throughout the whole protocol). Supernatant was removed, pellet was resuspended in 2 ml of CellWASH. Centrifugation, supernatant was removed and 0.5 ml of 1x Permeabilizing solution was added. Incubation at room temperature for 10 minutes. After centrifugation supernatant was removed and 2 ml of Rinse buffer was added. Tubes were put on vortex, centrifugation. Supernatant was removed and 40 µl of FC receptor saturation reagent prepared in blocking solution was added. Incubation at room temperature for 10 minutes. Cells were washed with 2 ml of Rinse buffered and centrifuged. This washing step was repeated one more time. Samples were divided into two sets. 40 µl of Isotype control were added to first and 40 µl of Primary Anti-Pgp Antibody were added to the second set. Incubation at room temperature for 30 minutes in dark. 2 ml of Rinse buffer were added to all samples, which were put on vortex and centrifuged. Supernatant was removed and 40 µl of Secondary FITC Antibody were added to all samples. Incubation at room temperature for 30 minutes in dark. 2 ml of Rinse buffer were added, centrifugation. Supernatant was removed and the pellets were resuspended in 500 µl of blocking solution.

Samples were kept in dark until analysis. The measurement was performed using flow cytometer, excitation at 488 nm, software CellQuest. The analysis of the measurements was performed using the ModFit program, version 2 (Verity Software House). Graphs, calculations and final analysis of the results were performed using Microsoft Excel® (Microsoft).

4.2.3.2 MRP1 analysis

For MRP1 analysis three samples from frozen stock cell suspension were prepared, each containing 2 million cells. Cell suspensions were transferred into cytometry tubes and centrifuged at room temperature, 500 *g* for 5 minutes (these centrifugation parameters were the same throughout the whole protocol). Supernatant was removed and 1 ml of 1x Permeabilizing solution was added. Incubated at room temperature for 10 minutes. 2 ml of Rinse buffer were added, and the samples were

divided into two sets. After centrifugation supernatant was removed. 100 µl of Isotype control were added to one set and 100 µl of Primary MRP1 Antibody were added to the second set. Incubation at room temperature for 60 minutes in dark. Cells were washed in 2 ml of Rinse buffer, put on vortex and centrifuged. Supernatant was removed and 100 µl of Secondary FITC Antibody diluted in Rinse buffer incl NP-40 were added to all samples. Incubation at room temperature for 30 minutes in dark. 2 ml of Rinse buffer were added, and the samples were centrifuged. Supernatant was removed and 0.5 ml of Rinse buffer was added.

The measurement was performed using flow cytometer, excitation at 488 nm, software CellQuest. The analysis of the measurements was performed using the ModFit program, version 2 (Verity Software House). Graphs, calculations and final analysis of the results were performed using Microsoft Excel® (Microsoft).

4.2.3.3 Phosphorylation of Histone H3P^{Ser10} analysis

For the Phosphorylation of Histone detection three samples from frozen stock cell suspension were prepared, each containing 2 million cells. Cell suspensions were transferred into cytometry tubes and centrifuged at room temperature, 800 *g* for 5 minutes (these centrifugation parameters were the same throughout the whole protocol). Supernatant was removed and 2 ml of 1% FBS in 1x PBS buffer were added. Supernatant was removed and 1 ml of cold 1x PBS + 0.25% Triton X-100 buffer was added during vortex. Incubation for 15 minutes on ice. Samples were centrifuged and the supernatant was removed. Cells were washed with 2 ml of 1% FBS in 1x PBS buffer and centrifuged. After supernatant was removed, 100 µl of Primary Anti-phospho-Histone H3 Antibody were added. Incubation at room temperature for 60 minutes in dark. After 30 minutes of incubation samples were put on vortex. 2 ml of 1% FBS in 1x PBS buffer were added and the samples were centrifuged. Supernatant was removed and 100 µl of Secondary Alexa Fluor 488 Antibody were added. Incubation at room temperature for 30 minutes in dark. 2 ml of 1% FBS in 1x PBS buffer were added and the samples were centrifuged. Supernatant was removed and 600 µl of Propidium iodide with RNase were added. Incubation at 37 °C in waterbath for 30 minutes in dark.

The measurement was performed using flow cytometer, excitation at 488 nm, software CellQuest. The analysis of the measurements was performed using the ModFit

program, version 2 (Verity Software House). Graphs, calculations and final analysis of the results were performed using Microsoft Excel® (Microsoft).

5 RESULTS

5.1 IC_{50} values of iron chelators

Using MTS assay, IC_{50} values of iron chelators were calculated for both HCT116 and CCRF-CEM cell lines. VLX600 IC_{50} for cell line HCT116 was 0.1 $\mu mol \cdot l^{-1}$ and for cell line CCRF-CEM 0.33 $\mu mol \cdot l^{-1}$. IC_{50} of XYZ iron chelator for HCT116 cell line was 2.68 $\mu mol \cdot l^{-1}$ and for CCRF-CEM cell line 0.46 $\mu mol \cdot l^{-1}$. All IC_{50} values for both iron chelators and both cell lines are summarized in **Table 1** with calculated standard deviations (SD). MTS assays were done in three replicates. Only the IC_{50} values $<1\ \mu mol \cdot l^{-1}$ were considered significant for the compounds activity. VLX600 iron chelator was used for the development of resistance in both cell lines, while for XYZ only CCRF-CEM cell line was selected and not the HCT116 cell line, as it had less significant IC_{50} value.

Table 1: IC_{50} values of VLX600 and XYZ iron chelators for HCT116 and CCRF-CEM cell lines with calculated standard deviations.

Cell line	Iron Chelator	IC_{50} [$\mu mol \cdot l^{-1}$]	SD
HCT116	VLX600	0.10	0.02
	XYZ	2.68	0.43
CCRF-CEM	VLX600	0.33	0.13
	XYZ	0.46	0.01

5.2 Determination of drug resistance

When the cells started growing in the presence of compounds, MTS assay was performed to determine the concentrations of drugs that the cell lines became resistant to. In CCRF-CEM cell line IC_{50} values for both iron chelators remained at the same values as for the parental cell line (**Fig. 7**). Both ways mentioned in Methods section and shown at **Fig. 6** did not lead to the development of resistance.

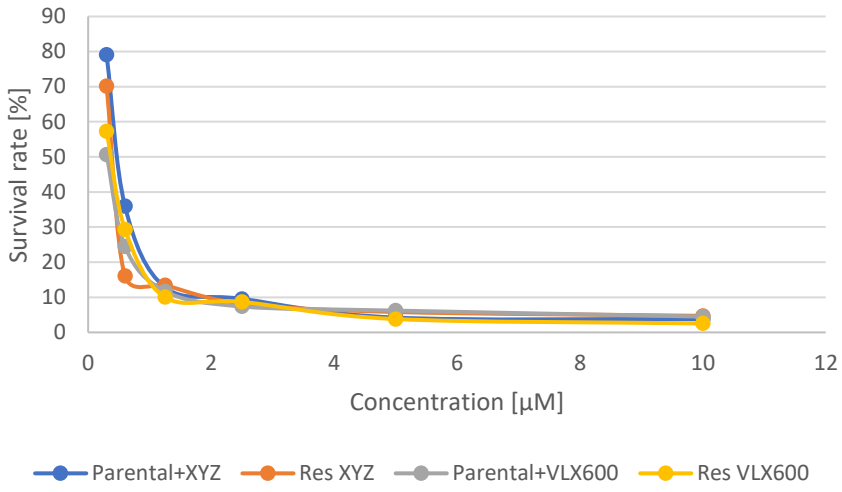

Figure 7: MTS assays after development of resistance in CCRF-CEM cell line. No significant changes in IC_{50} values of both iron chelators were registered, therefore no resistance was developed.

However, nine-fold increase in the IC_{50} value was observed with VLX600 iron chelator in HCT116 cell line (**Fig. 8**). MTS assay was done three times to confirm the resistance. This resistant cell line was used for further characterization using flow cytometry.

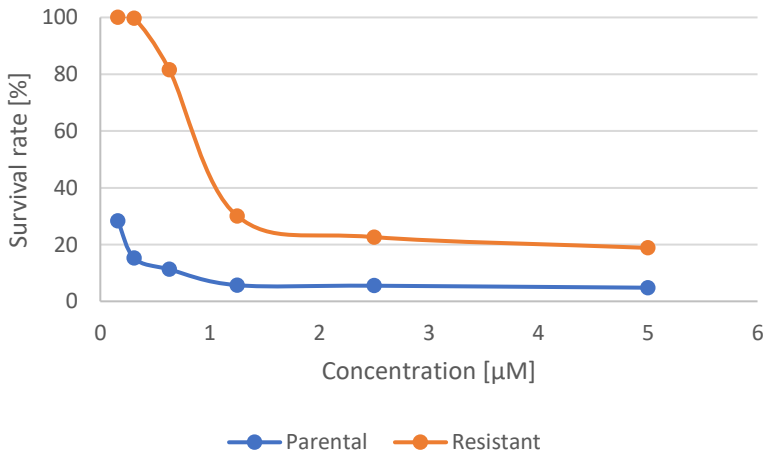

Figure 8: MTS assays of parental and VLX600 resistant HCT116 cell lines to determine the increase of IC_{50} in the resistant cells.

5.3 Characterization of drug resistance using flow cytometry

5.3.1 Pgp analysis

Considering a fact that Pgp, which belongs to the ABC transporter family, is usually responsible for MDR, flow cytometry analysis was performed. Both parental and resistant cell lines as well as untreated and treated cells were included to measure the expression of Pgp. In the cell populations an 1.75 increase in the expression of Pgp was observed in untreated resistant cells compared to parental cell line. After VLX600 treatment the Pgp expression was increased 1.9 times in the parental cell line. In the resistant cell line, it remained at the same level (**Fig. 9A**). This may be due to the maximal expression of Pgp in the resistant clones. In Pgp positive population the expression was 18% higher in parental cell line after treatment (**Fig. 9B**). Also, more Pgp positive cells were registered and a population shift was observed after VLX600 treatment (**Fig. 10**).

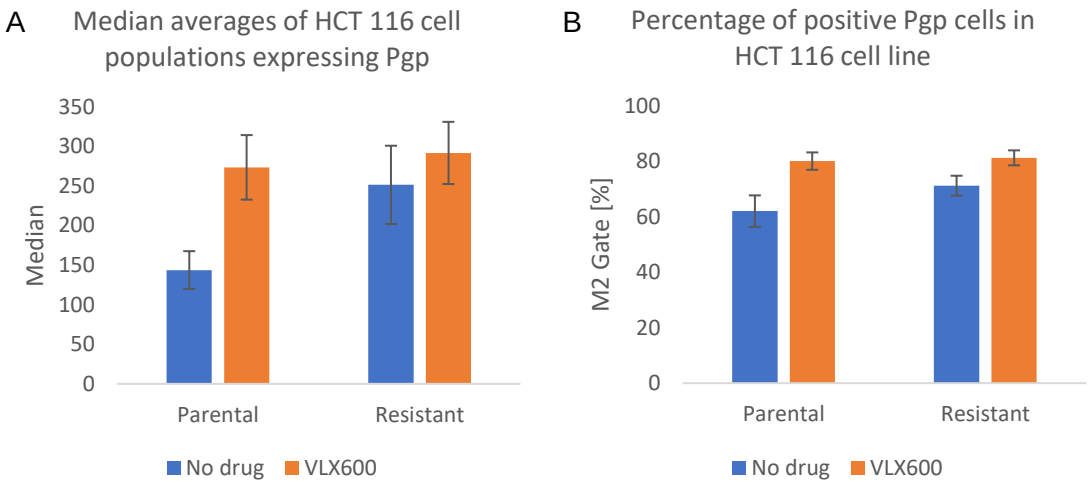

Figure 9: Pgp expression analysis in parental and resistant HCT116 cell lines. Treated cells were exposed to the VLX600 for 24 hours before analysis. Analysed data are from three independent experiments. **A** Average median values of the whole cell populations. **B** Percentage of positive cell populations expressing Pgp.

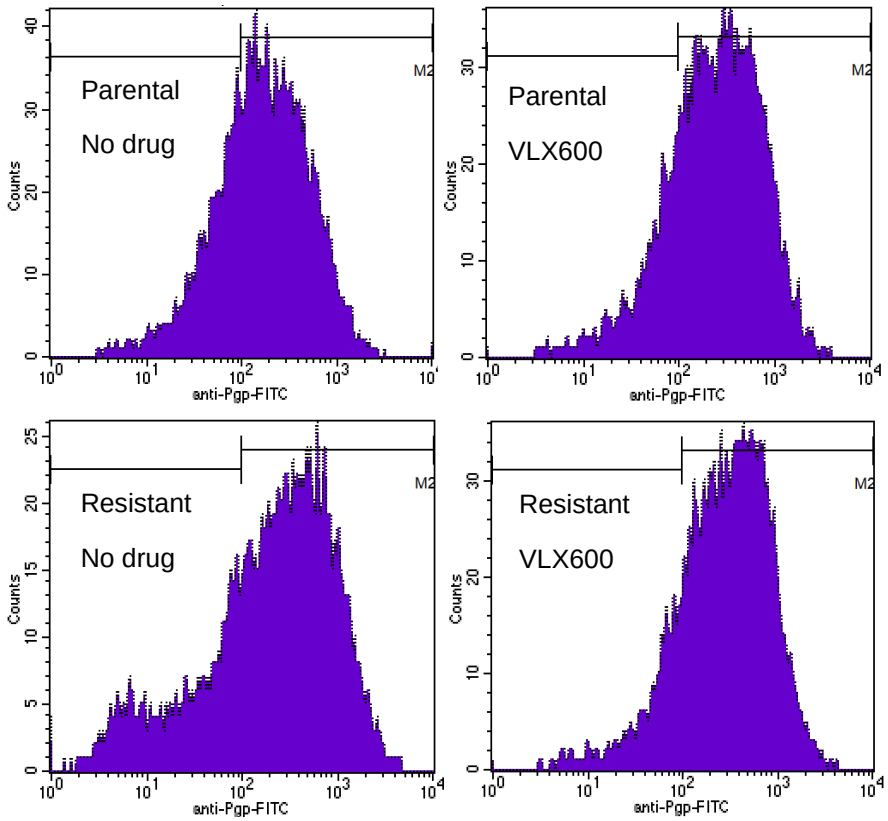

Figure 10: Histograms showing cell populations expressing Pgp. Population shift after VLX600 treatment can be seen in both parental and resistant cell lines. A representative graph from three independent experiments is shown for each measurement.

5.3.2 MRP1 analysis

MRP1 is another protein responsible for MDR in cancer and expression analysis of this protein was performed as well. The measurements were performed on both untreated and treated parental and resistant cell lines. An increased expression was observed in resistant cells in comparison to the parental cells in the whole cell populations. The expression was 1.3 times higher. After VLX600 treatment the expression was elevated 1.4 times in the parental cell line and remained at the same level in resistant cells (**Fig. 11A**). The explanation could be the maximal expression in the resistant cell line, where it reached its limit. In MRP1 positive cell populations the expression was increased by 16% in resistant cells in comparison to the parental cell line (**Fig. 11B**). A population shift was observed after treatment in parental cells, but no major differences were seen in the resistant cell line (**Fig. 12**).

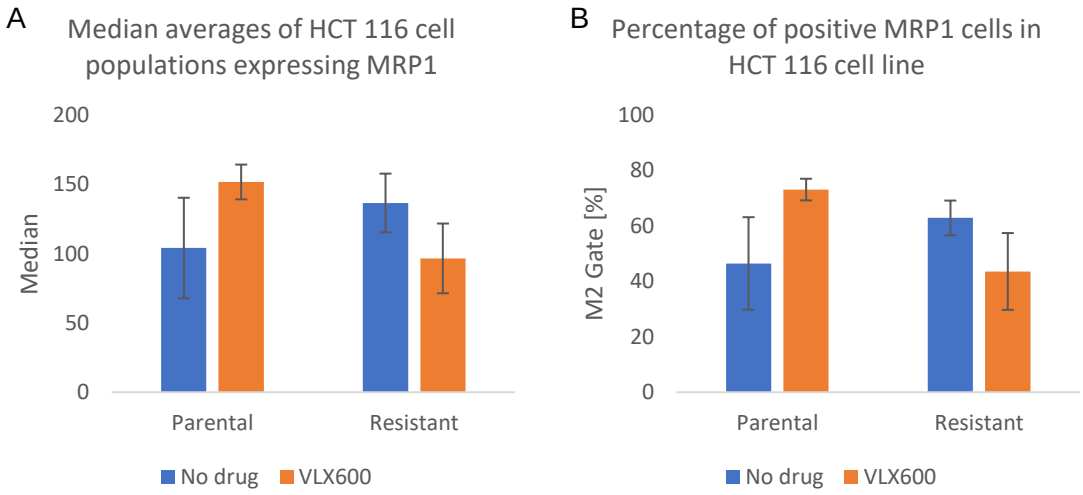

Figure 11: MRP1 expression analysis in parental and resistant HCT116 cell lines. Treated cells were exposed to the VLX600 for 24 hours before analysis. Analysed data are from three independent experiments. **A** Average median values of the whole cell populations. **B** Percentage of positive cell populations expressing MRP1.

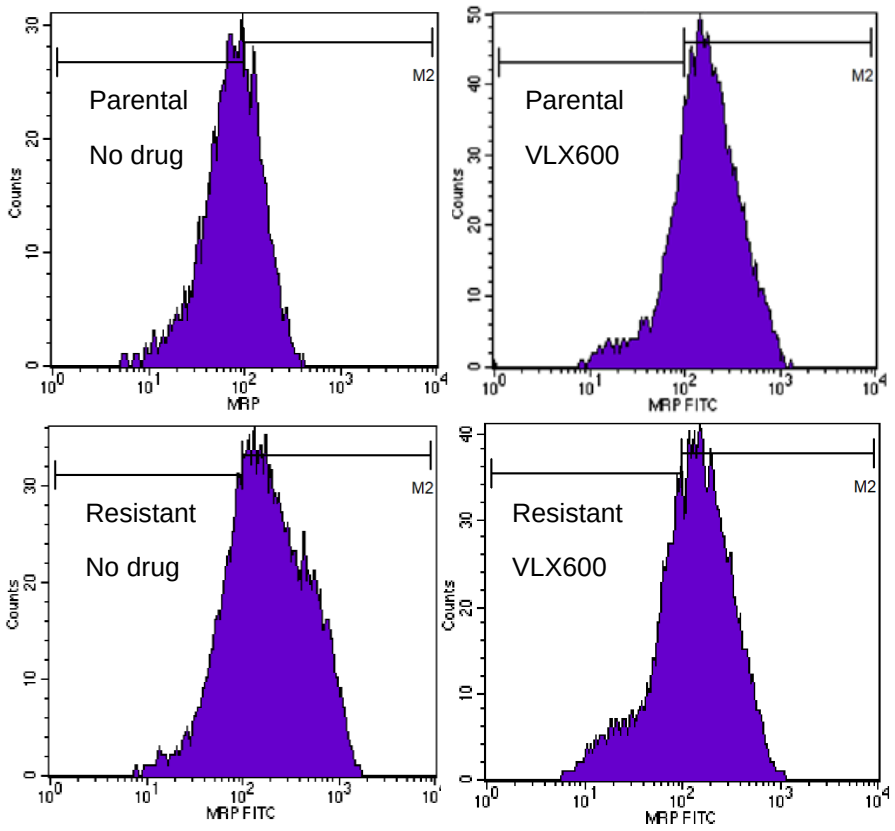

Figure 12: Histograms showing cell populations expressing MRP1. A population shift can be seen in the parental cell line. A representative graph from three independent experiments is shown for each measurement.

5.3.3 Cell cycle, Phosphorylation of Histone H3P^{Ser10} and Apoptosis analysis

The effect of drug resistance and the VLX600 treatment on the cell cycle was measured by flow cytometry. In the presence of VLX600 a higher number of both parental and resistant cells present in G2/M phase was observed and lower number in G0/G1 phase (**Table 2**). This elevation in G2/M phase was 15% in both cell lines. Number of cells in the S phase was unchanged. No additional changes were registered.

Table 2: Percentage of HCT116 cells in specific stages of the cell cycle with standard deviations. Data are the average of three independent experiments.

	Parental No Drug	SD	Parental VLX600	SD	Resistant No Drug	SD	Resistant VLX600	SD
G0/G1	33,74	1,48	21,11	1,43	35,17	1,29	18,71	0,36
S	43,48	2,45	41,59	1,43	42,82	0,73	43,79	0,96
G2/M	22,77	1,91	37,30	1,07	22,01	1,72	37,49	0,73

Because of serine10 phosphorylation in the tails of histone H3, that correlates with chromosome condensation in mitosis, it is possible to measure the amount of cells in the M phase of cell cycle. An increase of 0.6% was observed between untreated parental and resistant cells. In the presence of VLX600 in resistant cell line a decrease of 1.7% of cells in mitosis was registered (**Table 3**).

Table 3: Average values of HCT116 cell populations in mitosis with standard deviations. Data are the average of three independent experiments.

	H3P^{Ser10} [%]	SD
Parental No Drug	2,64	0,05
Parental VLX600	2,28	0,18
Resistant No Drug	3,21	0,07
Resistant VLX600	1,52	0,16

Analysis of subG1 population of cells, which is typical for apoptosis, was performed as well. Only a slight increase of 0.7% was registered between untreated parental and resistant cell line and a decrease of 1.1% in the presence of VLX600 in the resistant cells (**Table 4**).

Table 4: Average values of HCT116 subG1 cell populations with standard deviations. Data are the average of three independent experiments.

	SubG1 population [%]	SD
Parental No Drug	3,70	0,94
Parental VLX600	3,65	0,30
Resistant No Drug	4,46	0,04
Resistant VLX600	3,39	0,21

6 DISCUSSION

Multidrug resistance in cancer is a major medical issue and research seeks to overcome this problem in a variety of ways that include understanding the molecular mechanisms of the development of resistance, targeted or combined therapy, use of newly synthesized substances based on *in silico* simulations, etc. This thesis was focused on development of resistant cancer cell lines to the metal chelators and its characterization. Because iron is an essential nutrient, contributes to metastasis (52) and is even more common in tumour than in healthy cells, iron chelators are one of the possible choices for anticancer therapy.

Development of drug resistant cancer cell lines using metal chelating compounds has been partially successful. Two iron chelators were chosen for the development of resistance: XYZ and VLX600. XYZ iron chelator is an experimental compound synthesized by a collaborative chemist laboratory and it is under patent protection. It was not used for the development of resistance in HCT116 cell line due to its high IC_{50} value (2.68 $\mu mol \cdot 1^{-1}$). On the other hand, its low IC_{50} value in CCRF-CEM cell line (0.46 $\mu mol \cdot 1^{-1}$) served as a promising factor for development of resistance, which was not successful. This result indicates the possibility of using the compound as a potential anticancer drug to which tumour cells have difficulty developing a resistance.

The second chosen iron chelator, VLX600, was used for development of resistance in both cancer cell lines. Same as for XYZ iron chelator, no resistance was developed in CCRF-CEM cell line. Nevertheless nine-fold resistance was developed in HCT116 cells despite the low IC_{50} value (0.1 $\mu mol \cdot 1^{-1}$). This IC_{50} value was 19 times lower than previously reported (30). Characterization of the resistance using flow cytometry demonstrated a higher expression of Pgp and MRP1 in resistant cells. These findings confirm the role of ABC transporters in MDR in cancer (11,53,54). There were no changes in the morphology of resistant cell line as compared to the parental.

A genetic level analysis will confirm whether the cells have become genetically resistant. We did not perform any genetic level studies thus the resistance could be only temporary and environmentally dependent. However, the resistance was at the same level even after freezing and thawing the cells.

In addition, higher Pgp expression in resistant cells is a very basic mechanism of drug resistance and common for most of the drugs and cell lines. It does not necessarily

indicate the main cause of resistance. A knock down of *MDR1* gene, which produces Pgp, in resistant cells followed by expression analysis would serve as a confirmation of this hypothesis. Western blot analysis is another method that would confirm the expression of Pgp and its main role in the resistance.

There are very few studies on the development of resistance against metal chelators. This thesis shows promising effects of both chosen compounds. No resistance was developed in CCRF-CEM cell line and both iron chelators had low IC_{50} values. VLX600 resistant cancer cell line was developed in HCT116 cells, but there was a low IC_{50} value as well. These findings confirm the positive properties of VLX600 which is already in clinical studies (32). In conclusion, the iron chelators XYZ and VLX600 represent an option in combination with other anticancer drugs to overcome MDR.

7 CONCLUSIONS AND FUTURE PERSPECTIVES

Understanding the mechanisms of drug resistance in cancer is a crucial goal to overcome this treatment complication. One of the ways that can help to achieve it is the development of drug resistant cancer cell lines in the laboratory conditions. This aim of the thesis was partially fulfilled. VLX600 resistant HCT116 cell line was successfully developed with nine-fold increase in IC_{50} value. Flow cytometry analysis findings showed higher expression of Pgp and MRP1 in the resistant cells. However, further studies are needed to confirm the role of Pgp and MRP1 as causes of resistance.

Development of resistant CCRF-CEM cell lines was not successful with XYZ or VLX600 iron chelators. This may serve as a good example of positive and promising properties of metal chelators as potential anticancer drugs, to which tumours hardly become resistant. It is possible that they will be used in combination with other approaches, such as targeted Pgp inhibitors (55) or novel thiosemicarbazones (56) to overcome multiple drug resistance in cancer.

8 REFERENCES

1. Bray F, Ferlay J, Soerjomataram I, Siegel RL, Torre LA, Jemal A. Global cancer statistics 2018: GLOBOCAN estimates of incidence and mortality worldwide for 36 cancers in 185 countries. CA Cancer J Clin [Internet]. 2018 [cited 2019 Aug 2];68(6); p. 394–424. Available from: http://doi.wiley.com/10.3322/caac.21492

2. Ferlay J, Colombet M, Soerjomataram I, Dyba T, Randi G, Bettio M, et al. Cancer incidence and mortality patterns in Europe: Estimates for 40 countries and 25 major cancers in 2018. Vol. 103, European Journal of Cancer. Elsevier Ltd; 2018. p. 356–87.

3. Linehan WM, Rathmell WK. Kidney cancer. Vol. 30, Urologic Oncology: Seminars and Original Investigations. NIH Public Access; 2012. p. 948–51.

4. Felsenstein M, Hruban RH, Wood LD. New Developments in the Molecular Mechanisms of Pancreatic Tumorigenesis. Vol. 25, Advances in Anatomic Pathology. Lippincott Williams and Wilkins; 2018. p. 131–42.

5. Winterbourn CC. Toxicity of iron and hydrogen peroxide: the Fenton reaction. Vol. 82-83, Toxicol Lett. 1995. p. 969–74.

6. Inoue S, Kawanishi S. Hydroxyl radical production and human dna damage induced by ferric nitrilotriacetate and hydrogen peroxide. 47: Cancer Res. 1987; p. 6522–7.

7. Nemeth E, Tuttle MS, Powelson J, Vaughn MD, Donovan A, Ward DMV, et al. Hepcidin regulates cellular iron efflux by binding to ferroportin and inducing its internalization. 80- Science [Internet]. 2004 [cited 2020 Apr 11];306(5704); p. 2090–3. Available from: http://www.ncbi.nlm.nih.gov/pubmed/15514116

8. Torti S V., Torti FM. Iron and cancer: More ore to be mined. Vol. 13, Nature Reviews Cancer. Nature Publishing Group; 2013. p. 342–55.

9. Watts RN, Hawkins C, Ponka P, Richardson DR. Nitrogen monoxide (NO)-mediated iron release from cells is linked to NO-induced glutathione efflux via multidrug resistance-associated protein 1. 103(20), Proc Natl Acad Sci USA; 2006. p. 7670–5.

10. Robey RW, Pluchino KM, Hall MD, Fojo AT, Bates SE, Gottesman MM. Revisiting the role of ABC transporters in multidrug-resistant cancer. Vol. 18, Nature Reviews Cancer. Nature Publishing Group; 2018. p. 452–64.

11. Kathawala RJ, Gupta P, Ashby CR, Chen ZS. The modulation of ABC transporter-mediated multidrug resistance in cancer: A review of the past decade. Vol. 18, Drug Resistance Updates. Churchill Livingstone; 2015. p. 1–17.

12. Thelander L, Gräslund A, Thelander M. Continual presence of oxygen and iron required for mammalian ribonucleotide reduction: possible regulation mechanism. Biochem Biophys Res Commun [Internet]. 1983 [cited 2020 May 5];110(3); p. 859–65. Available from: http://www.ncbi.nlm.nih.gov/pubmed/6340669

13. Richardson DR. Iron chelators as therapeutic agents for the treatment of cancer. 42(3); Crit Rev Oncol Hematol; 2002. p. 267–81.

14. Gao J, Richardson DR. The potential of iron chelators of the pyridoxal isonicotinoyl hydrazone class as effective antiproliferative agents, IV: The mechanisms involved in inhibiting cell-cycle progression. 98(3); Blood; 2001. p. 842–50.

15. Kastan MB, Canman CE, Leonard CJ. P53, cell cycle control and apoptosis: Implications for cancer. (1); Cancer Metastasis Rev; 1995. p. 3–15.

16. Fukuchi K, Watanabe H, Kaetsu S, Gomi K, Tomovasu S, Tsuruoka N. Iron deprivation results in an increase in p53 expression. Biol Chem Hoppe Seyler [Internet]. 1995 [cited 2020 May 10];376(10); p. 627–36. Available from: https://www.degruyter.com/view/j/bchm3.1995.376.issue-10/bchm3.1995.376.10.627/bchm3.1995.376.10.627.xml

17. Donfrancesco A, Deb G, Dominici C, Pileggi D, Castello MA, Helson L. Effects of a Single Course of Deferoxamine in Neuroblastoma Patients. 50(16); Cancer Res; 1990. p. 4929–30.

18. Dezza L, Cazzola M, Danova M, Carlo-Stella C, Bergamaschi G, Brugnatelli S, et al. Effects of desferrioxamine on normal and leukemic human hematopoietic cell growth: In vitro and in vivo studies. 3(2); Leukemia; 1989. p. 104–7.

19. Hann HL, Stahlhut MW, Rubin R, Maddrey WC. Antitumor effect of deferoxamine on human hepatocellular carcinoma growing in athymic nude mice. 70(8); Cancer; 1992. p. 2051–6.

20. Oexle H, Gnaiger E, Weiss G. Iron-dependent changes in cellular energy metabolism: Influence on citric acid cycle and oxidative phosphorylation. 1413(3); Biochim Biophys Acta - Bioenerg; 1999. p. 99–107.

21. Selig RA, White L, Gramacho C, Sterling-Levis K, Fraser IW, Naidoo D. Failure of Iron Chelators to Reduce Tumor Growth in Human Neuroblastoma Xenografts. 58(3); Cancer Research; 1998. p. 473–478.

22. F Wang, RL Elliot, JF Head. Inhibitory effect of deferoxamine mesylate and low iron diet on the 13762NF rat mammary adenocarcinoma. 19(1A); Anticancer Res; 1999. p. 445–50.

23. Cappellini MD, Taher A. Deferasirox (Exjade®) for the treatment of iron overload. Vol. 122, Acta Haematologica. 2009. p. 165–73.

24. Ohyashiki JH, Kobayashi C, Hamamura R, Okabe S, Tauchi T, Ohyashiki K. The oral iron chelator deferasirox represses signaling through the mTOR in myeloid leukemia cells by enhancing expression of REDD1. 100(5); Cancer Sci; 2009. p. 970–7.

25. Vazana-Barad L, Granot G, Mor-Tzuntz R, Levi I, Dreyling M, Nathan I, et al. Mechanism of the antitumoral activity of deferasirox, an iron chelation agent, on mantle cell lymphoma. 54(4); Leuk Lymphoma; 2013. p. 851–9.

26. Knox JJ, Hotte SJ, Kollmannsberger C, Winquist E, Fisher B, Eisenhauer EA. Phase II study of Triapine® in patients with metastatic renal cell carcinoma: A trial of the National Cancer Institute of Canada Clinical Trials Group (NCIC IND.161). 25(5); Invest New Drugs; 2007. p. 471–7.

27. Traynor AM, Lee JW, Bayer GK, Tate JM, Thomas SP, Mazurczak M, et al. A phase II trial of Triapine® (NSC# 663249) and gemcitabine as second line treatment of advanced non-small cell lung cancer: Eastern Cooperative Oncology Group Study 1503. 28(1); Invest New Drugs; 2010. p. 91–7.

28. Green DA, Wong SJ, Chitambar CR, Antholine WE, Richardson DR. Inhibition of malignant cell growth by 311, a novel iron chelator of the pyridoxal isonicotinoyl hydrazone class: Effect on the R2 subunit of ribonucleotide reductase. 7(11); Clin Cancer Res; 2001. p. 3574–9.

29. Gao J, Lovejoy D, Richardson DR. Effect of iron chelators with potent anti-proliferative activity on the expression of molecules involved in cell cycle progression and growth. 4(6); Redox Rep; 1999. p. 311–2.

30. Fryknäs M, Zhang X, Bremberg U, Senkowski W, Olofsson MH, Brandt P, et al. Iron chelators target both proliferating and quiescent cancer cells. 6(1); Sci Rep; 2016. p. 1–11.

31. Zhang X, Fryknäs M, Hernlund E, Fayad W, De Milito A, Olofsson MH, et al. Induction of mitochondrial dysfunction as a strategy for targeting tumour cells in metabolically compromised microenvironments. 5(1); Nat Commun; 2014. p. 1–14.

32. Mody K, Mansfield AS, Vemireddy L, Nygren P, Gulbo J, Borad M. A phase I study of the safety and tolerability of VLX600, an Iron Chelator, in patients with refractory advanced solid tumors. Invest New Drugs [Internet]. 2019 [cited 2019 Oct 2];37(4); p. 684–92. Available from: http://link.springer.com/10.1007/s10637-018-0703-9

33. Housman G, Byler S, Heerboth S, Lapinska K, Longacre M, Snyder N, et al. Drug Resistance in Cancer: An Overview. Cancers (Basel) [Internet]. 2014 [cited 2019 Jan 30];6(3); p. 1769–92. Available from: http://www.mdpi.com/2072-6694/6/3/1769

34. Sauna ZE, Ambudkar SV. Characterization of the catalytic cycle of ATP hydrolysis by human P-glycoprotein. The two ATP hydrolysis events in a single catalytic cycle are kinetically similar but affect different functional outcomes. J Biol Chem [Internet]. 2001 [cited 2020 May 13];276(15); p. 11653–61. Available from: http://www.ncbi.nlm.nih.gov/pubmed/11154703

35. Saraswathy M, Gong S. Different strategies to overcome multidrug resistance in cancer. 31(8); Biotechnol Adv; 2013. p. 1397–407.

36. Cole SPC, Sparks KE, Fraser K, Loe DW, Grant CE, Wilson GM, et al. Pharmacological Characterization of Multidrug Resistant MRP-transfected Human Tumor Cells. 54(22); Cancer Res; 1994. p. 5902–10.

37. Ejendal KF, Hrycyna CA. Multidrug Resistance and Cancer: The Role of the Human ABC Transporter ABCG2. 3(5); Curr Protein Pept Sci; 2005. p. 503–11.

38. Sampath D, Cortes J, Estrov Z, Du M, Shi Z, Andreeff M, et al. Pharmacodynamics of cytarabine alone and in combination with 7-hydroxystaurosporine (UCN-01) in AML blasts in vitro and during a clinical trial. 107(6); Blood; 2006. p. 2517–24.

39. Michael M, Doherty MM. Tumoral drug metabolism: Overview and its implications for cancer therapy. 23(1); J Clin Oncol; 2005. p. 205–29.

40. Gibson P, Gill JH, Khan PA, Seargent JM, Martin SW, Batman PA, et al. Cytochrome P450 1B1 (CYP1B1) Is Overexpressed in Human Colon Adenocarcinomas Relative to Normal Colon: Implications for Drug Development. 2(6); Mol Cancer Ther; 2003. p. 527–34.

41. Rodriguez-Antona C, Ingelman-Sundberg M. Cytochrome P450 pharmacogenetics and cancer. Vol. 25, Oncogene. Nature Publishing Group; 2006. p. 1679–91.

42. Zwelling LA, Ledley FD, Mayes J, Altschuler E, Zwelling LA. Identification of a Point Mutation in the Topoisomerase II Gene from a Human Leukemia Cell Line Containing an Amsacrine-resistant Form of Topoisomerase II. 51(17); Cancer Res; 1991. p. 4729–31.

43. Gorre ME, Mohammed M, Ellwood K, Hsu N, Paquette R, Nagesh Rao P, et al. Clinical resistance to STI-571 cancer therapy caused by BCR-ABL gene mutation or amplification. 293(5531); Science (80-); 2001. p. 876–80.

44. Navin N, Krasnitz A, Rodgers L, Cook K, Meth J, Kendall J, et al. Inferring tumor progression from genomic heterogeneity. 20(1); Genome Res; 2010. p. 68–80.

45. Cros J, Raffenne J, Couvelard A, Poté N. Tumor Heterogeneity in Pancreatic Adenocarcinoma. 85(1–2); Pathobiology; 2018. p. 64–71.

46. Li W, Zhang H, Assaraf YG, Zhao K, Xu X, Xie J, et al. Overcoming ABC transporter-mediated multidrug resistance: Molecular mechanisms and novel therapeutic drug strategies. Vol. 27, Drug Resistance Updates. Churchill Livingstone; 2016. p. 14–29.

47. Kakarla P, Inupakutika M, Devireddy AR, Gunda SK, Willmon TM, Ranjana KC, et al. 3D-QSAR and contour map analysis of tariquidar analogues as multidrug resistance protein-1 (MRP1) inhibitors. 7(2); Int J Pharm Sci Res; 2016. p. 554–572.

48. Aggarwal BB, Kumar A, Bharti AC. Anticancer potential of curcumin: Preclinical and clinical studies. Vol. 23, Anticancer Research. 2003. p. 363–98.

49. Yan YD, Kim DH, Sung JH, Yong CS, Choi HG. Enhanced oral bioavailability of docetaxel in rats by four consecutive days of pre-treatment with curcumin. 399(1–2); Int J Pharm; 2010. p. 116–20.

50. Choi JS, Piao YJ, Kang KW. Effects of quercetin on the bioavailability of doxorubicin in rats: Role of CYP3A4 and P-gp inhibition by quercetin. 34(4); Arch Pharm Res; 2011. p. 607–13.

51. Duan Z, Brakora KA, Seiden M V. Inhibition of ABCB1 (MDR1) and ABCB4 (MDR3) expression by small interfering RNA and reversal of paclitaxel resistance in human ovarian cancer cells. Mol Cancer Ther [Internet]. 2004 [cited 2020 May 17];3(7); p. 833–8. Available from: http://www.ncbi.nlm.nih.gov/pubmed/15252144

52. Leng X, Wu Y, Arlinghaus RB. Relationships of lipocalin 2 with breast tumorigenesis and metastasis. J Cell Physiol [Internet]. 2011 [cited 2020 Jun 8];226(2); p. 309–14. Available from: http://doi.wiley.com/10.1002/jcp.22403

53. Higgins CF. Multiple molecular mechanisms for multidrug resistance transporters. Vol. 446, Nature. Nature Publishing Group; 2007. p. 749–57.

54. Lu JF, Pokharel D, Bebawy M. MRP1 and its role in anticancer drug resistance. Vol. 47, Drug Metabolism Reviews. Taylor and Francis Ltd; 2015. p. 406–19.

55. Nanayakkara AK, Follit CA, Chen G, Williams NS, Vogel PD, Wise JG. Targeted inhibitors of P-glycoprotein increase chemotherapeutic-induced mortality of multidrug resistant tumor cells. 8(1); Sci Rep; 2018. p. 1–18.

56. Pati ML, Niso M, Ferorelli S, Abate C, Berardi F. Novel metal chelators thiosemicarbazones with activity at the σ2 receptors and P-glycoprotein: An innovative strategy for resistant tumor treatment. 5(125); RSC Adv; 2015. p. 103131–46.

APPENDIX

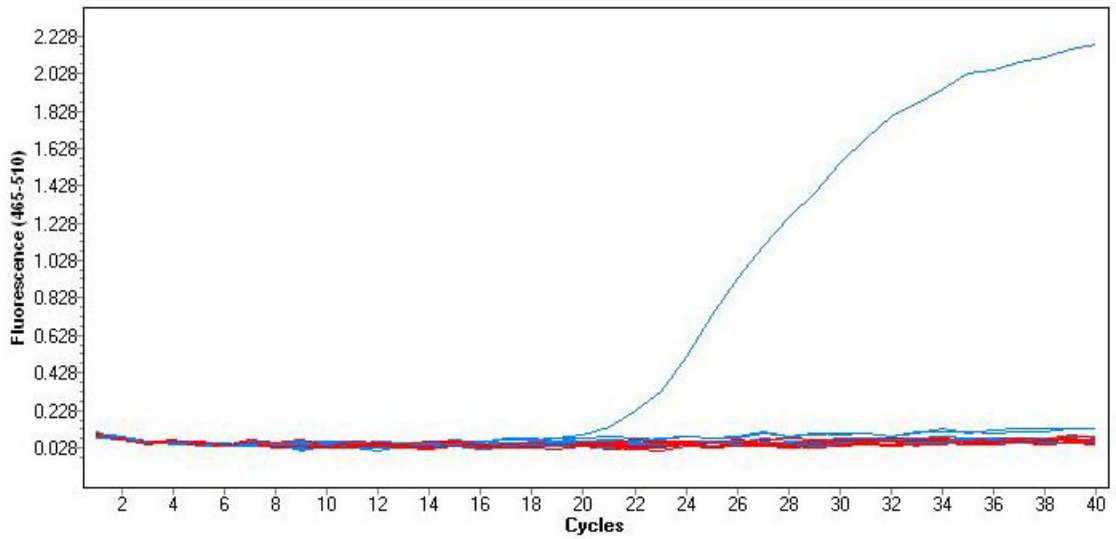

Mycoplasma testing for cell culture contamination using qPCR. Testing was performed every two weeks. The positive control is shown by a blue curve. The rest of the samples is negative.